physica status solidi

www.pss-journals.com

reprint

WILEY-VCH

Phys. Status Solidi A **209**, No. 8, 1432–1437 (2012) / **DOI** 10.1002/pssa.201127682

physica status solidi a
www.pss-a.com
applications and materials science

Contact-free reactions between micropipes in bulk SiC growth

Mikhail Yu. Gutkin[1,2,3], Alexander G. Sheinerman[1], Victor G. Kohn[4], Tatiana S. Argunova[5,6], Mikhail A. Smirnov[2], and Jung Ho Je*[,6]

[1] Institute of Problems in Mechanical Engineering, RAS, Bolshoy 61, Vasilievskii Ostrov, 199178 St. Petersburg, Russia
[2] Department of Physics of Materials Strength and Plasticity, St. Petersburg State Polytechnical University, Polytekhnicheskaya st. 29, 195251 St. Petersburg, Russia
[3] Department of Theory of Elasticity, St. Petersburg State University, Universitetskii 28, Stary Petergof, 198504 St. Petersburg, Russia
[4] Russian Research Center 'Kurchatov Institute', Kurchatov sq. 1, 123182 Moscow, Russia
[5] Ioffe Physical-Technical Institute, RAS, Polytekhnicheskaya st. 26, 194021 St. Petersburg, Russia
[6] Department of Materials Science and Engineering, Pohang University of Science and Technology, San 31 Hyoja-dong, Namku, 790–784 Pohang, Republic of Korea

Received 18 November 2011, revised 26 March 2012, accepted 19 April 2012
Published online 14 May 2012

Keywords crystal structure, defects, single crystal growth, synchrotron X-ray diffraction

* Corresponding author: e-mail jhje@postech.ac.kr, Phone: +82-054-2798081, Fax: +82-054-2792992

It has been generally accepted that any reaction between micropipes in silicon carbide (SiC) crystals requires a direct contact of the micropipes. We propose a new model of contact-free reactions that are realized through the emission and absorption of full-core dislocations by micropipes. This model can explain the correlated reduction in micropipe radii in the samples with low micropipe densities which has been observed in synchrotron radiation (SR) phase contrast images supported by computer simulations. We provide a theoretical description of a contact-free reaction between two parallel micropipes.

1 Introduction Silicon carbide (SiC) single crystals grown by sublimation contain structural defects such as micropipes, dislocations, stacking faults, inclusions, etc. Many efforts have been spent in recent years to elucidate the technologies of industrial production of high quality SiC crystals. These efforts have given good results. For example, 4H-SiC, with micropipe densities as low as 0.7 cm^{-2} over a full 100 mm diameter of the crystals were grown [1]. However, for large current devices, even smaller micropipe density of less than 0.5–0.1 cm^{-2} is required. This is because the increase in device power is achieved through extension of the device area; however, even one micropipe can destroy a device [2]. Hence, the micropipe problem still remains rather important when dealing with bulk SiC single crystals.

Micropipes are known to nucleate at screw dislocations, inclusions, and foreign polytype boundaries [3–5]. Therefore, the elimination of these defects causes the reduction of the micropipes density [6–9]. Moreover, the micropipe density decreases when micropipes react between themselves and with other structural defects. They can dissociate into full-core dislocations [10–12]; react with each other [13, 14] and with foreign polytype inclusions [15]. The structural transformations (in particular, annihilation and healing) of micropipes resulting from such reactions as well as generation of new micropipes from slit-like microvoids [16] determine micropipe density at final stages of crystal growth. Thus, a reaction between micropipes is always a positive process in view of their elimination from growing SiC crystals. Therefore, one should understand better the mechanisms of reactions between micropipes and the factors stimulating such reactions.

In our earlier research (see Ref. [14] for a review), we focused on micropipe reactions which occur when micropipes come in contact, touching each other by their surfaces. Let us call this kind of reactions as "contact reactions". Figure 1 illustrates such a contact reaction between two micropipes, MP1 and MP2, which contain opposite-sign superscrew dislocations with Burgers vectors $\boldsymbol{b}_1$ and $\boldsymbol{b}_2$, respectively. Due to elastic attraction of opposite dislocations, the micropipes gradually shift to each other during the crystal growth, react and produce a new micropipe MP3 containing a new superscrew dislocation with the sum

Original Paper

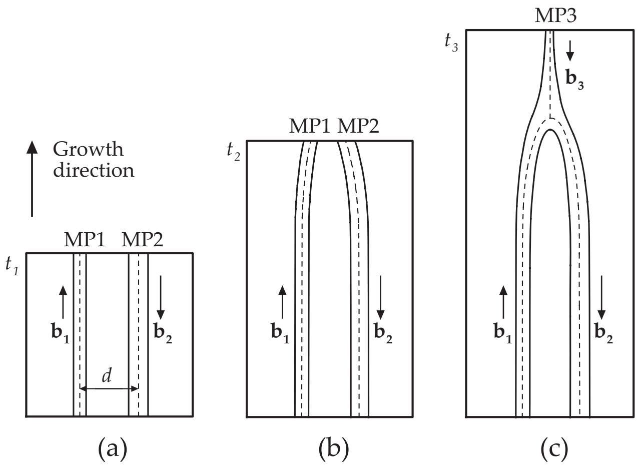

Figure 1 Sketch of the contact reaction between micropipes MP1 and MP2 in a longitudinal section of growing SiC crystal in sequential moments of time t_i. (a) Initial state at the moment of time t_1. The micropipes contain superscrew dislocations with opposite Burgers vectors $\boldsymbol{b}_1$ and $\boldsymbol{b}_2$. (b) Intermediate state at the moment of time $t_2 > t_1$. The micropipes gradually shift to each other. (c) Final state at the moment of time $t_3 > t_2$. The micropipes meet each other and react, forming a new micropipe MP3 that contains a superscrew dislocation with the sum Burgers vector $\boldsymbol{b}_3 = \boldsymbol{b}_1 + \boldsymbol{b}_2$.

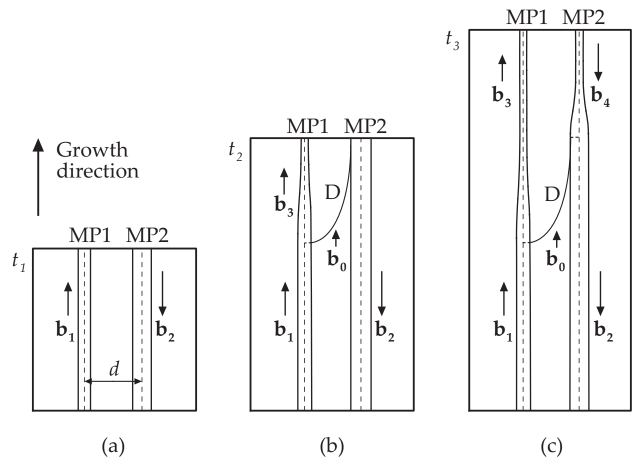

Figure 2 Sketch of the contact-free reaction between micropipes MP1 and MP2 in a longitudinal section of a growing SiC crystal in sequential moments of time t_i. (a) Initial state at the moment of time t_1. The micropipes contain superscrew dislocations with opposite Burgers vectors $\boldsymbol{b}_1$ and $\boldsymbol{b}_2$. (b) Intermediate state at the moment of time $t_2 > t_1$. Micropipe MP1 emits a quarter-loop of full-core dislocation D with Burgers vector $\boldsymbol{b}_0$. As a result, the Burgers vector of MP1 changes from $\boldsymbol{b}_1$ to $\boldsymbol{b}_3 = \boldsymbol{b}_1 - \boldsymbol{b}_0$, and the radius of MP1 decreases. Dislocation D shifts from MP1 to MP2; the frontal (top) segment of D is absorbed by MP2. (c) Final state at the moment of time $t_3 > t_2$. Micropipe MP2 changes its Burgers vector from $\boldsymbol{b}_2$ to $\boldsymbol{b}_4 = \boldsymbol{b}_2 + \boldsymbol{b}_0$, and, as a consequence, also decreases its radius.

Burgers vector $\boldsymbol{b}_3 = \boldsymbol{b}_1 + \boldsymbol{b}_2$, $b_3 < (b_1, b_2)$, where b_i is the Burgers vector magnitude, $i = 1, 2, 3$. As the micropipe radius is in the quadratic dependence on its Burgers vector magnitude [17], the profit of this reaction is evident: instead of two micropipes we get only one with a much smaller radius. In the special case of $b_3 = b_0$, where b_0 is the Burgers vector magnitude of the elemental full-core dislocation, micropipe MP3 is normally healed.

Although the contact reactions between micropipes are highly effective for diminishing their density; however, these reactions become less probable when the micropipe density decreases. Recently, we have suggested another form of micropipe reactions, which does not need a contact between micropipe surfaces and can occur through an exchange of full-core dislocations (*i.e.*, conventional screw dislocations whose lines are not surrounded by voids) [20]. We call this kind of reactions as "contact-free reactions". Figure 2 gives a sketch of the contact-free reaction between the same micropipes, MP1 and MP2 [Fig. 2(a)], as shown in Fig. 1(a). During the crystal growth, micropipe MP1 emits a full-core dislocation quarter-loop D which expands, reaches the surface of micropipe MP2 [Fig. 2(b)] and reacts with its dislocation [Fig. 2(c)]. The corresponding dislocation reactions are described by equations: $\boldsymbol{b}_1 - \boldsymbol{b}_0 = \boldsymbol{b}_3$ and $\boldsymbol{b}_2 + \boldsymbol{b}_0 = \boldsymbol{b}_4$, where $\boldsymbol{b}_3$ and $\boldsymbol{b}_4$ are the Burgers vectors of micropipes MP1 and MP2, respectively, after the contact-free reaction. The profit of this reaction is that both the micropipe radii decrease, the MP1's one after the emission of the full-core dislocation, while the MP2's one after its absorption [Fig. 2(c)]. Strong decrease in micropipe radii can lead to their gradual healing.

The suggested contact-free reaction between micropipe requires the motion of dislocation quarter-loops from one micropipe to another one. The problem is that full-core screw dislocations with rather high Burgers vector magnitude ($b_0 = 1$ nm in 4H-SiC and 1.5 nm in 6H-SiC) can hardly glide in usual sense. A commonly accepted view is that such dislocations are sessile. However, the motion of dislocation quarter-loops near a micropipe during the growth of a 6H-SiC crystal has been documented by Sugiyama et al. [18] through etching and polishing the grown crystal from the surface to the inside successively. They revealed that screw dislocations shifted outwards from the micropipe as the growth proceeded. They indicated that medium etch pits characterizing the lateral positions of screw dislocations shifted outwards for 3–10 and 10–40 μm during the vertical growth of 60 and 200 μm, respectively. This points to the formation and expansion of dislocation quarter-loops in the vicinity of a micropipe. Also, Siche et al. [19] observed a couple of micropipes "which act as dislocation sources and dislocations are distributed around them" (see Fig. 2 in Ref. [19]). It is worth noting that the authors did not mean here the basal dislocations. In opposite, they emphasized that "Between neighboring micropipes the dislocations are partly aligned (Fig. 2). This could be one of the reasons for the generation of short slits," which open between the micropipes in the plane where the micropipes lie. These observations also support the idea that micropipes can emit dislocation quarter-loops having screw dislocation segments parallel with the micropipes. The mechanism of shift of the sessile full-core screw dislocation is still not perfectly clear. One can speculate that this process proceeds just under the surface of growing crystal, where the dislocation glide is much easier than in the bulk of the crystal, and occurs through a step-by-step mechanism including a glide of a short-length screw dislocation segment over an elementary interatomic distance and an elongation of this dislocation segment with the crystal growth.

In our paper [20], we demonstrated the experimental evidence of a micropipe configuration similar to that shown in Fig. 2, when two neighboring micropipes reduce their diameters (approximately by half) one after another, at different distances from the surface of a grown crystal. This can be treated as an indirect proof of the contact-free reaction. Indeed, the distance difference shows that there exists an intervening time between the emission and absorption events, when the emitted dislocation covers the distance between the micropipes. Such an idea appeared when we observed micropipes in SiC by using synchrotron white X-ray beam [20]. Few micropipes had variable cross-sections which were evaluated via a computer simulation of the phase contrast images based on the Kirchhoff technique with a real X-ray spectrum taken into account [21, 22]. These experimental observations and computer simulations allowed us to conclude that the contact-free reaction can be a real process which is capable to noticeably affect the evolution of micropipe ensemble and to cause a decrease in micropipe density. However, due to space limitations, we had no possibility to discuss our theoretical model in detail. In particular, we did not show any formula in support of its possible reality. The main purpose of this paper is to consider our model in detail with special attention to the conditions necessary for the contact-free reaction. For the sake of completeness, we also show some results of our experimental observations and computer simulations.

2 Model

Let us perform a theoretical analysis of the necessary conditions for contact-free reactions between micropipes. Recently, the possibility for the emission of a dislocation from a micropipe at the crystal growth front has been analyzed within a three-dimensional model [23]. The model geometry was rather similar to that shown in Fig. 2; however, without the second micropipe (MP2). The presence of the second micropipe makes the three-dimensional model very complicated for a correct analytical examination. That is why here we use a simplified two-dimensional model of a contact-free reaction between two parallel micropipes to catch mainly some principal qualitative results.

Consider micropipes MP1 and MP2 with circular cross-sections of the radii r_1 and r_2 that contain screw dislocations with the Burgers vectors $\boldsymbol{b}_1 = b_1\boldsymbol{e}_z$ and $\boldsymbol{b}_2 = b_2\boldsymbol{e}_z$, respectively, where $\boldsymbol{e}_z$ is the unit vector in the direction of the z-axis (Fig. 3). The distance between the micropipe axes is denoted as d. Let the first micropipe emit a screw full-core dislocation with the Burgers vector $\boldsymbol{b}_0$. We also assume that a shear stress $\tau^0 = \tau^0_{yz}$ associated with thermal stresses appearing during

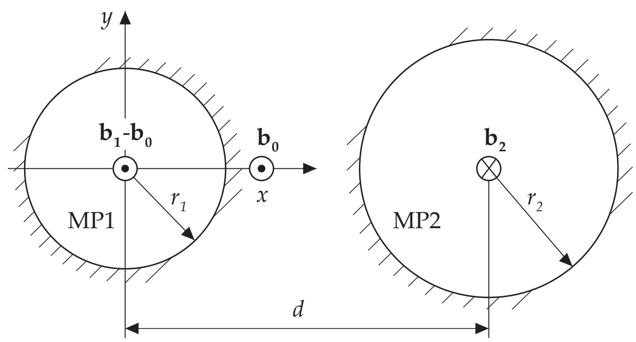

Figure 3 A model of contact-free reaction between two micropipes realized through screw dislocation exchange. Micropipe MP1 emits a dislocation with the Burgers vector $\boldsymbol{b}_0$, which shifts to micropipe MP2 and is absorbed by it.

the growth of SiC [24, 25] acts in the region between the examined MPs and far from their surfaces.

To analyze the possibility of such an emission event, we utilize the energy variation ΔW associated with dislocation emission. In our case of $d \gg r_1, r_2$, it is sufficient to separately consider the effects of the two voids on the shear stress as well as on the image force exerted by the micropipe surfaces on the emitted dislocation and the forces of dislocation interaction. In this approximation, the thermal shear stress τ_{yz} acting on the emitted dislocation in between the micropipes, taken with account for the stress concentration near their surfaces, is

$$\tau_{yz}(d \gg r_1, r_2) \approx \tau^0 \left(1 + \frac{r_1^2}{x^2} + \frac{r_2^2}{(d-x)^2} \right), \tag{1}$$

where x is the coordinate of the emitted dislocation. In formula (1), the second and third terms in brackets reflect the effects of the first and second void [26], respectively, in the limiting case $d \gg r_1, r_2$ when the mutual influence of the voids is negligible.

The total elastic force acting on the emitted dislocation (per its unit length) follows as

$$\begin{aligned} F(d \gg r_1,\, r_2) &\approx b_0\tau_{yz} \\ &+ \frac{Gb_0}{2\pi} \left\{ \frac{b_1 - b_0}{x} - \frac{b_2}{d-x} + \frac{b_0}{x} - \frac{b_0 x}{x^2 - r_1^2} \right. \\ &\left. - \frac{b_0}{d-x} + \frac{b_0(d-x)}{(d-x)^2 - r_2^2} \right\}, \end{aligned} \tag{2}$$

where G is the shear modulus. The first term in (2) denotes the force exerted by the external stress τ_{yz} given by (1). In brackets of formula (2), the first and second terms correspond to the interactions of the emitted dislocation with dislocations within micropipes MP1 and MP2, respectively; the third–fourth and fifth–sixth terms correspond to the image force [27, 28] exerted by the surface of MP1 and MP2, respectively.

The energy ΔW associated with dislocation emission (per unit length of the dislocation) is given by $\Delta W = \int_{r_1}^{x-b_0} F(x)\mathrm{d}x + W_\mathrm{c}$, where $W_\mathrm{c} \approx Gb_0^2/(4\pi)$ is the dislocation core energy [29]. Substitution of (1) and (2) to the latter relation for ΔW yields:

$$\Delta W = b_0\tau^0\left(x - \frac{r_1^2}{x} + \frac{r_2^2}{d-x} - \frac{r_2^2}{d-r_1}\right) + \frac{Gb_0^2}{4\pi}\left\{1 + \ln\frac{\left(x^2 - r_1^2\right)\left[(d-x)^2 - r_2^2\right]}{b_0 r_1 (d-x)^2} + \frac{2b_1}{b_0}\ln\frac{r_1}{x} + \frac{2b_2}{b_0}\ln\frac{d}{d-x}\right\}. \quad (3)$$

It is worth noting that formula (3) is valid in the limit of $d \gg r_1, r_2$ only (which is the case of the present work). When MPs are close enough (say, $d \leq r_1, r_2$), one should use a much more complicated expression for ΔW based on the strict solutions of boundary-value problems for screw dislocations inside two closely spaced micropipes [28] and in between of them [30]. It is rather cumbersome, so we do not show it here. However, we have utilized it to check the correctness of numerical calculations evaluated with approximation (3).

In the following calculations, we will use the Frank relation [17] $r_i = Gb_i^2/(8\pi^2\gamma)$ between the Burgers vectors magnitudes b_i and micropipe radii r_i, where γ is the surface energy. Numerical evaluation of ΔW for the case of growing 4H-SiC crystal with $G = 165$ GPa, $\gamma/G = 1.4 \times 10^{-3}$ nm [31] and equilibrium micropipes (for which the Frank relation [17] is valid) shows that ΔW depends primarily on the Burgers vectors of micropipe dislocations and on the level of thermal shear stress τ^0 (Fig. 4).

Let us first consider the case when $\tau^0 = 0$ [Fig. 4(a)]. As is seen, the dislocation exchange is most energetically favorable if the Burgers vectors $\boldsymbol{b}_1$ and $\boldsymbol{b}_2$ are opposite in sign. At the same time, to shift from one micropipe to the other, the emitted dislocation must overcome an energetic barrier. If the Burgers vectors of the two micropipes are of the same sign, the emitted dislocation must overcome two energetic barriers on its way from one micropipe to the other. In this case, the possibility for the dislocation exchange between these micropipes is governed by the difference of the Burgers vector magnitudes. If $(b_1 - b_2) < 3b_0$, then we have: $\Delta W > 0$, and the dislocation exchange is impossible. If $(b_1 - b_2 \geq 3b_0)$, then the dislocation reaction can occur if the emitted dislocation is able to overcome the two energetic barriers. The presence of two energetic barriers results in the appearance of an equilibrium position for the emitted dislocation, situated in between the micropipes.

Figure 4(b) shows the case where micropipes initially have the same Burgers vectors, equal in magnitude to $7b_0$, and the dislocation emission occurs under the action of a thermal shear stress τ^0. One can see that the stress τ^0 reduces the energetic barriers for the dislocation exchange. In the range of stress values from 10 to 100 MPa, which are

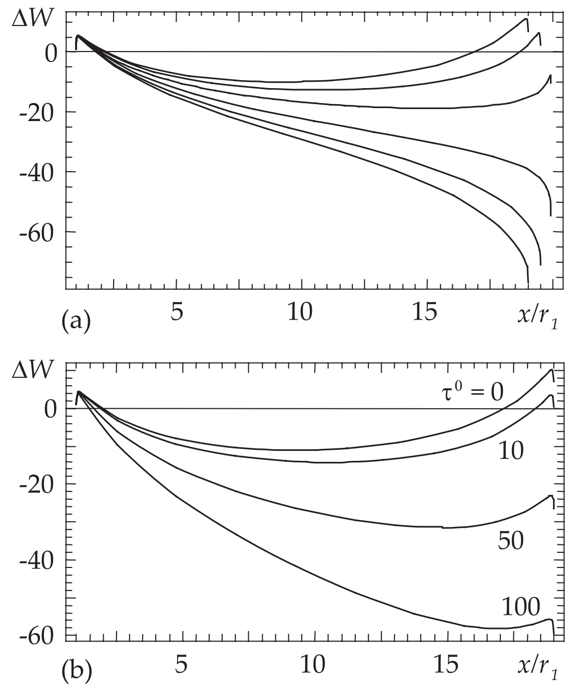

Figure 4 Dependences of the energy ΔW associated with the emission of a dislocation by a micropipe near a second micropipe on the normalized dislocation coordinate x/r_1 for $d/r_1 = 20$ and $b_1/b_0 = 7$. (a) $\tau^0 = 0$ and $b_2/b_0 = -7, -5, -2, 2, 5, 7$ (from bottom to top). (b) $b_2/b_0 = 7$ and $\tau^0 = 0, 10, 50$, and 100 MPa. The energy ΔW is given in units of $Gb_0^2/4\pi$, the stress values are given at the curves in MPa.

characteristic for bulk SiC growth [24, 25], the first barrier decreases weakly while the second one strongly. The first barrier has the height of about $1.5Gb_0^2/\pi$ per unit dislocation length, which for a 4H-SiC crystal with $G = 165$ GPa and $b_0 = 1$ nm gives $\approx 0.48Gb_0^2 l \approx 125$ eV per unit distance $l \approx 0.252$ nm [32] between basal atomic planes. This value is obviously very high that is not surprising due to the model of an infinite medium considered within the classical theory of linear elasticity. Moreover, in reality, the dislocation emission is expected to occur within a rather thin subsurface layer under the growth front where the conditions can be very far from equilibrium due to high temperature and surface effects. The height of the second barrier is approximately five times higher at $\tau^0 = 0$ but it falls down to $\approx 0.16Gb_0^2 l$ at $\tau^0 = 100$ MPa. The equilibrium position of the emitted dislocation increases from $\approx 9r_1$ at $\tau^0 = 0$ to $\approx 17r_1$ at $\tau^0 = 100$ MPa. One can conclude that thermal shear stress greatly promotes dislocation transfer and makes it possible even in the case of micropipes having large Burgers vectors of the same sign.

3 Experimental results

Phase contrast images of individual micropipes were obtained using white beam at a third generation synchrotron radiation (SR) source in Pohang, Korea. At 7B2 X-ray microscopy beamline of Pohang Light Source the beam from a bending magnet was created by a source with effective sizes of 160 (H) and 60 (V) μm, located at a distance of 34 m from the sample. CCD detector registered visible light produced by a crystal-scintillator $CdWO_4$ with the thickness 150 μm. The light after the crystal reflected from a silicon mirror and passed by the interchangeable lens system with magnification from 1× to 50×. The 14 bit gray scale matrix size was 1600 (H) × 1200 (V) pixels; the view field was 310 μm (H), and the minimal pixel size was 0.19 μm.

SiC sample was the plate cut off from the crystal 4H-SiC grown by the sublimation sandwich method [5] on the seed 6H-SiC (00.1). In the chamber with Ar atmosphere and Sn vapor the temperature was 2180 °C; and the growth rate was 0.35 mm/h. The Sn vapor caused the transformation of the polytype of the substrate into 4H-SiC [5]. The crystal was N doped up to 2×10^{18} cm^{-3}. The orientation of the sample surface was ($\bar{1}1.0$), so micropipes located almost parallel to the growth axis were nearly parallel to the surface. Micropipes grouped (with the density of ≈10^2 cm^{-2}) along the boundaries of foreign polytype inclusions (6H and 12R) which appeared at ≈1 cm distance from the seed/boule interface. Below the inclusions over the area of 1 cm^2 micropipes were undetectable.

The sample was fixed on the holder with its surface perpendicular to the beam and rotated to achieve a horizontal position of micropipe axes. So the images were measured by using the more coherent vertical projection of the source.

The phase contrast images of micropipes were with black edges and white inside. For few individual micropipes the distance between the edges modified along the axes showing that their cross-sections changed through the crystal. A good example is the micropipe group in Fig. 5. There are three micropipes forming the group: two in contact (the thickest, MP1, and the thinnest) and the third, MP2, lying remotely at the distance ≈130 μm from MP1. The image details of MP1 and MP2 demonstrate that their cross-sections are variable. Their diameters were determined through computer simulation.

Computer simulation of white beam phase contrast images requires a real SR spectrum forming an image. In white beam various harmonics are incoherent. However, the simulation can be done using the following observations. Firstly, various harmonics with different intensities exponentially decrease starting from 5 keV. Secondly, low energies are absorbed inside all objects in the beam path including the sample itself. As a result, the spectrum is confined to a limited energy range, and an image is effectively created via the summation of many patterns produced by harmonics taken with different weights. The theory and the algorithm were described in Refs. [21, 22]. Simulation program for a micropipe image was written in Java and ACL (Advanced Command Language) [33]. The experimental intensity profile was measured perpendicular to the pipe axis. The program read the normalized profile and deduced the starting values of the pipe diameters D and D_0 perpendicular and parallel to the beam. By sequential adjustment of D, D_0 one obtained the best match between

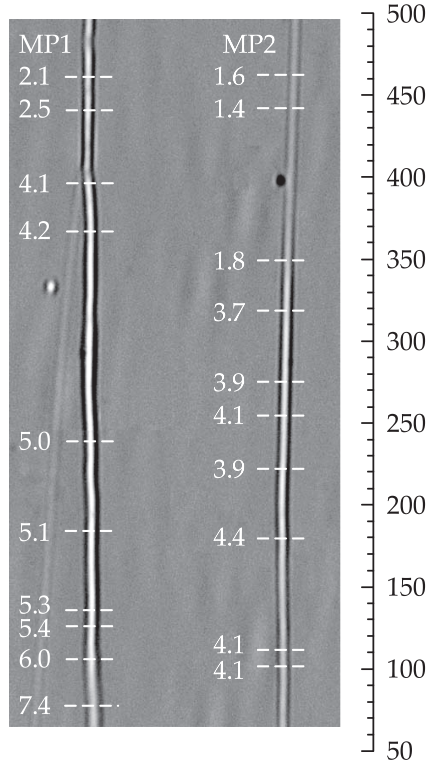

Figure 5 Phase contrast image of micropipes MP1 and MP2 in the interval of 70–500 μm along the pipe axes. Variation in transverse cross-section sizes along the lines of MP1 and MP2 are shown on the image (in μm). The sample-to-detector distance is 10 cm.

experiment and simulation. The cross-section cannot be obtained from one experimental measurement since the coherent image of a pipe varies with distance both in width as it broadens and also because its structure is variable. The simulation technique suggested in Refs. [21, 22] implies fitting the series of images recorded at different distances from the sample. The resulting deduced diameters D, D_0 are independent from the distance. In addition to the distance simulation we fitted the different cross-sections along the pipes axes in order to get the distribution of their sizes.

We found that the micropipes had elliptical cross-sections extended in transverse direction, i.e., perpendicular to the beam. The transverse diameters of micropipes MP1 and MP2 are presented in Fig. 5 versus the distance along the pipe axes increasing in the growth direction. It is seen that, with growth, the transverse size of MP1 reduces from 7.4 to 2.1 μm. At the same time, the transverse size of the MP2 reduces from 4.1 to 1.6 μm. In contrast, the longitudinal diameters remain almost the same and of the order of 0.8 μm for the MP1 and 0.5 μm for the MP2 (data not shown). In the correlated decrease of MP1 and MP2 cross-section sizes in Fig. 5 several features are apparent. A remarkable decrease of the MP1 cross-section size occurs in the distance interval from 74 to 132 μm while the transverse diameter of MP2 drastically decreases later in the distance interval from 314 to 345 μm. In addition, a rapid decrease of the transverse diameter of MP1 happens in the distance interval from 393 to 458 μm when the transverse diameter of MP2 remains almost invariable.

We explain the changes in the cross-sections of the two neighboring micropipes by the contact-free reaction between them. Experimental images in Fig. 5 tend to confirm the reaction schematically shown in Fig. 2. Most likely, during the rapid decrease of its cross-section area MP1 emits a full-core dislocation shifting toward MP2 and finally absorbed by it.

It is worth noting that the contact reaction between the thinnest micropipe and MP1 in Fig. 5 is rather similar to that shown schematically in Fig. 1.

4 Summary We have considered a new possible mechanism for the contact-free reactions between micropipes that are realized through the exchange of full-core dislocations. The emission or the absorption of an elementary screw dislocation by a micropipe result in the essential change of the micropipe radius. Our calculations have demonstrated that, depending on the signs of the micropipe Burgers vectors (prior to dislocation exchange between micropipes), the shifting dislocation must overcome one or two energetic barriers. In the case where the initial micropipe Burgers vectors are of the same sign, the dislocation exchange can happen only if the difference between the micropipe Burgers vector magnitudes is large enough (not less than three magnitudes of the elementary Burgers vector). The energetic barrier(s) that the dislocation has to surmount on its way from one micropipe to the other one can supposedly be overcome through thermal fluctuations. Also, the thermal shear stress greatly promotes dislocation transfer and makes it possible even in the case of micropipes with large Burgers vectors of the same sign. It is intuitively clear that the effect can occur with the MPs having elliptical as well as circular cross-sections.

Using SR phase contrast imaging, we have demonstrated the correlated reduction in the radii of two remote micropipes in SiC with low micropipe density. This effect indirectly supports our suggestion that micropipes can interact without a direct contact, by the mechanism of contact-free reaction which is realized through the exchange of full-core dislocations between the micropipes and leads to their further possible healing.

Acknowledgements This work was supported by the Creative Research Initiatives (Functional X-ray Imaging) of MEST/KOSEF of Korea and the Russian Ministry of Science and Education (grant MD-164.2012.1).

References

[1] St. G. Müller, M. F. Brady, A. A. Burk, H. McD. Hobgood, J. R. Jenny, R. T. Leonard, D. P. Malta, A. R. Powell, J. J. Sumakeris, V. F. Tsvetkov, and C. H. Carter, Jr., Superlattices Microstruct. **40**, 195 (2006).
[2] T. Hatakeyama, K. Ichinoseki, K. Fukuda, N. Higuchi, and K. Arai, J. Cryst. Growth **310**, 988 (2008).
[3] J. Heindl, H. P. Strunk, V. D. Heydemann, and G. Pensl, Phys. Status Solidi A **162**, 251 (1997).
[4] M. Dudley, X. R. Huang, W. Huang, A. Powell, S. Wang, and P. Neudeck, Appl. Phys. Lett. **75**, 784 (1999).
[5] Yu. A. Vodakov, A. D. Roenkov, M. G. Ramm, E. N. Mokhov, and Yu. N. Makarov, Phys. Status Solidi B **202**, 177 (1997).
[6] E. Schmitt, T. Straubinger, M. Rasp, M. Vogel, and A. Wohlfart, J. Cryst. Growth **310**, 966 (2008).
[7] N. Ohtani, M. Katsuno, H. Tsuge, T. Fujimoto, M. Nakabayashi, H. Yashiro, M. Sawamura, T. Aigo, and T. Hoshino, J. Cryst. Growth **286**, 55 (2006).
[8] J. L. Liu, J. Q. Gao, J. K. Cheng, J. F. Yang, and G. J. Qiao, J. Mater. Sci. **42**, 6148 (2007).
[9] P. Wu, M. Yoganathan, and I. Zwieback, J. Cryst. Growth **310**, 1804 (2008).
[10] I. Kamata, H. Tsuchida, T. Jikimoto, and K. Izumi, Jpn. J. Appl. Phys. **39**, 6496 (2000).
[11] B. M. Epelbaum and D. J. Hofmann, Cryst. Growth **225**, 1 (2001).
[12] R. Yakimova, N. Vouroutzis, M. Syväjärvi, and J. Stoemenos, J. Appl. Phys. **98**, 034905 (2005).
[13] X. Ma, J. Appl. Phys. **99**, 063513 (2006).
[14] M. Yu. Gutkin, A. G. Sheinerman, and T. S. Argunova, Phys. Status Solidi C **6**, 1942 (2009).
[15] M. Yu. Gutkin, A. G. Sheinerman, T. S. Argunova, J. M. Yi, J. H. Je, S. S. Nagalyuk, E. N. Mokhov, G. Margaritondo, and Y. Hwu, Phys. Rev. B **76**, 064117 (2007).
[16] T. S. Argunova, M. Yu. Gutkin, J. H. Je, E. N. Mokhov, S. S. Nagalyuk, and Y. Hwu, Phys. Status Solidi A **208**, 819 (2011).
[17] F. C. Frank, Acta Crystallogr. **4**, 497 (1951).
[18] N. Sugiyama, A. Okamoto, K. Okumura, T. Tani, and N. Kamiya, J. Cryst. Growth **191**, 84 (1998).
[19] D. Siche, H.-J. Rost, J. Doerschel, D. Schulz, and J. Wollweber, J. Cryst. Growth **237–239**, 1187 (2002).
[20] M. Yu. Gutkin, A. G. Sheinerman, M. A. Smirnov, V. G. Kohn, T. S. Argunova, J. H. Je, and J. W. Jung, Appl. Phys. Lett. **93**, 151905 (2008).
[21] V. G. Kohn, T. S. Argunova, and J. H. Je, Appl. Phys. Lett. **91**, 171901 (2007).
[22] T. Argunova, V. Kohn, J. W. Jung, and J. H. Je, Phys. Status Solidi A **206**, 1833 (2009).
[23] M. Yu. Gutkin and A. G. Sheinerman, Phys. Status Solidi B **241**, 1810 (2004).
[24] St. G. Müller, R. C. Glass, H. M. Hobgood, V. F. Tsvetkov, M. Brady, D. Henshall, J. R. Jenny, D. Malta, and C. H. Carter, Jr., J. Cryst. Growth **211**, 325 (2000).
[25] R. H. Ma, H. Zhang, M. Dudley, and V. Prasad, J. Cryst. Growth **258**, 318 (2003).
[26] A. R. Thölén, Acta Metall. **18**, 445 (1970).
[27] P. Pirouz, Philos. Mag. A **78**, 727 (1998).
[28] M. Yu. Gutkin and A. G. Sheinerman, Phys. Status Solidi B **231**, 356 (2002).
[29] J. P. Hirth and J. Lothe, Theory of Dislocations (Wiley, New York, 1982).
[30] M. Yu. Gutkin, A. G. Sheinerman, and M. A. Smirnov, Mech. Mater. **41**, 905 (2009).
[31] W. Si, M. Dudley, R. Glass, V. Tsvetkov, and C. Carter, Jr., J. Electron. Mater. **26**, 128 (1997).
[32] M. Dudley, X. R. Huang, and W. M. Vetter, J. Phys. D: Appl. Phys. **36**, A30 (2003).
[33] See http://vkacl.narod.ru for the programming language ACL.